

Facts and Artifacts in the Blinking Statistics of Semiconductor Nanocrystals

Catherine H. Crouch,^{*,†} Orion Sauter,[†] Xiaohua Wu,[‡] Robert Purcell,[†] Claudia Querner,[§] Marija Drndic,[§] and Matthew Pelton[‡]

[†]Department of Physics and Astronomy, Swarthmore College, Swarthmore, Pennsylvania 19081, ^{*}Center for Nanoscale Materials, Argonne National Laboratory, Argonne, Illinois 60439, and [§]Department of Physics and Astronomy, University of Pennsylvania, Philadelphia, Pennsylvania 19104

ABSTRACT Since its initial discovery just over a decade ago, blinking of semiconductor nanocrystals has typically been described in terms of probability distributions for durations of bright, or “on,” states and dark, or “off,” states. These distributions are obtained by binning photon counts in order to construct a time series for emission intensity and then applying a threshold to distinguish on states from off states. By examining experimental data from CdSe/ZnS core/shell nanocrystals and by simulating this data according to a simple, two-state blinking model, we find that the apparent truncated power-law distributions of on times can depend significantly on the choices of binning time and threshold. For example, increasing the binning time by a factor of 10 can double the apparent truncation time and change the apparent power-law exponent by 30%, even though the binning time is only 3% of the truncation time. Our findings indicate that stringent experimental conditions are needed to accurately determine blinking-time probability distributions. Similar considerations should apply to any phenomenon characterized by time series data that displays telegraph noise.

KEYWORDS Semiconductor nanocrystals, blinking statistics, truncated power-law distribution

The ability to measure fluorescence from individual emitters has revealed interesting and important phenomena that are obscured in measurements of macroscopic ensembles. A central example is the tendency of many fluorophores, including single molecules, fluorescent proteins, and semiconductor nanocrystals in the shape of spheres, rods, and wires, to switch irregularly under continuous illumination between bright states and dark states.^{1–5} Colloidally synthesized semiconductor nanocrystals (NCs) provide a particularly convenient system to study this fluorescence intermittency, or “blinking,” because of their high quantum yield, broad absorption bands, and stability against photobleaching. Furthermore, understanding and eliminating blinking^{4–6} is crucial for the development of biomedical and optoelectronic applications involving NCs.

Widespread interest in NC blinking was stimulated by the unexpected observation just over a decade ago that the durations of bright and dark periods, or “on” and “off” states, follow power-law statistics over many orders of magnitude, from microseconds up to seconds or even minutes.^{7–10} These power-law statistics are most commonly characterized by determining distributions, $P(t_{\text{on}})$ and $P(t_{\text{off}})$, for “on” and “off” periods, respectively.^{7,11} In practice, the intensity of light emitted by a single NC is collected as a function of time, either through a linear detector such as a CCD camera or by time-resolved single-photon counting. An intensity-time series is constructed by integrating the measured

intensity (or the number of detected photons) over time bins of fixed width; that is, one calculates $I_n = \int_{(n-1)\Delta t}^{n\Delta t} I(t) dt$, where Δt is the width of the time bins, $I(t)$ is the detected intensity (or number of photons counted) at time t , and the number n runs from the beginning to the end of the experiment. An intensity threshold I_{th} is chosen such that the NC is said to be “on” when $I_n > I_{\text{th}}$ and is said to be “off” when $I_n < I_{\text{th}}$. If I_n remains below I_{th} for n sequential time bins, then $t_{\text{off}} = n\Delta t$ is taken to be the duration of a single off period. A normalized histogram of all such off periods is taken to represent the off-time probability distribution $P(t_{\text{off}})$; the on-time distribution $P(t_{\text{on}})$ is determined in a similar way.

Many such measurements have established that the off-time distribution follows a power law, $P(t_{\text{off}}) = At_{\text{off}}^{-m_{\text{off}}}$, for at least six decades in time.⁷ The on-time distributions, on the other hand, follow a power law for durations from milliseconds up to at most several seconds, but then drop off more rapidly, following a truncated power-law distribution $P(t_{\text{on}}) = At_{\text{on}}^{-m_{\text{on}}} e^{-t_{\text{on}}/\tau_{\text{on}}}$.¹² The qualitative dependence of the truncation time, τ_{on} (also known as the “saturation time”), on temperature, intensity, and nanocrystal size was reported in one of the earliest studies of NC blinking.¹⁰ More recent studies have explored the quantitative dependence of both τ_{on} and the exponent m_{on} on excitation intensity,^{13–17} environment,^{13,16} NC shape,¹⁴ the number of NCs in a cluster,¹⁸ and excitation wavelength.^{15,19–21}

All these studies involved choosing a binning time, Δt , for construction of a time series, choosing a threshold level, I_{th} , for construction of the on-time distribution and fitting the resulting distribution, usually using a least-squares procedure. This method is inherently problematic though, because

*To whom correspondence should be addressed. E-mail: ccrouch1@swarthmore.edu. Phone: (610) 328-8386. Fax: (610) 328-7895.

Received for review: 01/5/2010

Published on Web: 04/05/2010



it introduces an artificial time scale to the analysis.²² If a NC blinks on and off several times during a single binning time, these separate, short blinking periods will be mistaken for one, longer period; whether this period is considered to be “on” or “off” will depend on the choice of I_{th} compared to the average emitted intensity during the binning time. This effect can be mitigated by reducing Δt ; however, this increases the effects of shot noise and instrumental noise, eventually making it impossible to distinguish photons emitted from the NC from background light and dark counts in the detector. It has previously been noted that the choice of bin size can introduce distortions in exponential blinking-time distributions,²³ that is, distributions described by a single characteristic blinking time, as in the case of many molecules, and a general theoretical description of this case has been developed.²⁴ Here, we consider the power-law and truncated-power-law distributions that are generally observed for semiconductor nanocrystals.

Previous investigations into the effects of binning and thresholding on the blinking statistics of semiconductor nanocrystals have focused primarily on the off-time distributions. Measurements⁸ and simulations^{12,25} both indicate that the power-law distributions are unaffected by changes in Δt over at least 2 orders of magnitude. Similarly, the distributions are relatively insensitive to changes in I_{th} , provided it is set significantly above the background level.^{18,26,27} Qualitatively, the robustness of the power-law distribution can be attributed to its self-similar nature: because the power law has no characteristic time scale, it is not strongly affected by the introduction of an artificial binning time. The truncated power law that describes the on-time distribution, on the other hand, has an intrinsic time scale, defined by τ_{on} . It is reasonable to suppose that, if Δt is similar to this characteristic time, then significant distortion of the distribution will occur.²³ So far, few studies have been made of potential artifacts in on-time distributions, and those few have focused on the effect of the threshold level.^{16,27} Varying I_{th} over a limited range, similar to the values typically used, was found to not significantly affect the calculated distributions.¹⁸ Varying the threshold over a much wider range, on the other hand, produces large changes in apparent values of τ_{on} and m_{on} . This sensitivity to I_{th} was recently used to motivate a model of blinking involving multiple emitting states.²⁷

Here, we examine the effect of choices made in analyzing blinking data in order to distinguish facts from artifacts in studies of single-emitter blinking. We report the critical importance of both bin time and threshold in determining on-time probability distributions for spherical and rod-shaped core-shell nanocrystals. Both the truncation time τ_{on} and the power-law exponent m_{on} are affected. We observe this sensitivity of $P(t_{on})$ to bin time and threshold, not only for experimental data, but also for simulated data that assumes a simple two-level system with power-law-distributed off times and truncated-power-law-distributed on times. Furthermore, the effects of binning and thresholding

are interrelated, with binning being of primary importance. This study identifies the stringent experimental requirements, both for the signal-to-noise ratio and the number of recorded events, needed for accurate determination of on-time probability distributions. The study also reveals that, for some single-emitter data, it is impossible to confidently obtain the underlying distribution. Since trends in values of τ_{on} and m_{on} are important for comparison between experiment and theory, the insights of this work are relevant for a broad range of other nanoscale blinking emitters.

To examine how bin time affects the on-time probability distributions obtained from experimental data, we measure the photon emission rate from individual nanocrystals using a standard epi-fluorescence configuration; details on the sample preparation and measurement are given in the Supporting Information. Figure 1a shows an intensity-time series from a representative core-shell nanocrystal, excited with 100 W/cm² of continuous-wave laser light with a wavelength of 443 nm, using a bin time $\Delta t = 3$ ms.

To obtain distributions of on and off times from the time series, we must choose a threshold intensity, I_{th} . One approach is to construct a histogram of intensity values, as illustrated in Figure 1b. When the histogram consists of two distinct peaks, I_{th} can be set at the minimum between the two peaks, as illustrated in the figure; we refer to this as the “center threshold”. Alternatively, the threshold can be set based on statistical analysis of the background count rate, determined by isolating a dark (“off”) region of the binned time trace $I(t)$. A commonly used method in the blinking literature is to determine the mean value and standard deviation for the background level, and then set the threshold a certain number of standard deviations above the mean.^{7,8,24,28} Here, we use an alternative threshold definition, by assuming the background counts are described by Poisson statistics, and then setting I_{th} equal to the highest possible count rate that could be represented in the background over the duration of the experiment.²⁹ This “Poisson threshold,” although still phenomenological, is expected to eliminate nearly all false blinking events induced by noise. The corresponding threshold levels are also illustrated in Figure 1b.

Once the threshold has been chosen, intensity data are converted to a sequence of on and off times. From this sequence, we then determine the probability distribution of off or on events. These probability distributions are most commonly analyzed using least-squares fitting, so we adopt the same method here.

In order to produce a probability distribution that can be analyzed using least-squares fitting, we apply the statistical weighting scheme introduced by Kuno et al.⁷

$$P(t_{off(on)}) = \frac{N(t_{off(on)})}{N_{off(on)}^{tot}} \frac{1}{\delta t_{off(on)}^{avg}} \quad (1)$$

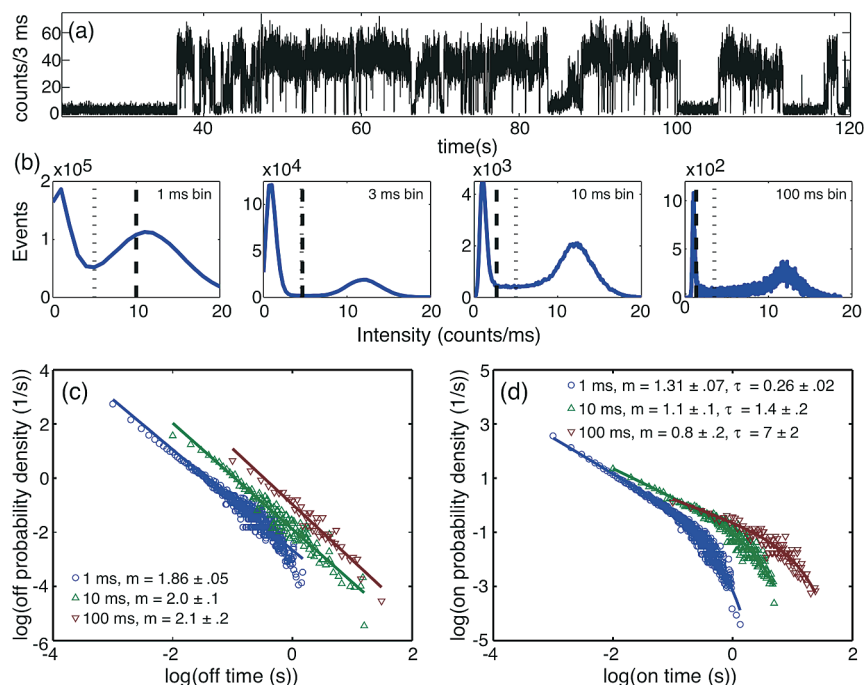


FIGURE 1. (a) Representative excerpt from an intensity time trace, $I(t)$, obtained from a single nanocrystal, using binning time $\Delta t = 3$ ms. The total duration of the experiment was 1800 s. (b) Histograms of intensities obtained from the entire duration of the data set excerpted in (a), for $\Delta t = 1, 3, 10$, and 100 ms. The Poisson threshold is shown by the heavy dashed line and the center threshold by the dotted line (see text for threshold definitions). (c) Weighted off-time probability distributions, $P(t_{\text{off}})$, obtained using center thresholding, for different values of Δt (see text for explanation of weighting method). Points are experimental values, and lines are the results of least-squares fitting. (d) Weighted on-time probability distribution, $P(t_{\text{on}})$, together with least-squares fitting results.

where $N(t_{\text{off(on)}})$ is the number of off (on) events of duration $t_{\text{off(on)}}$, $N_{\text{off(on)}}^{\text{tot}}$ is the total number of off (on) events observed in the time series, and $\delta t_{\text{off(on)}}^{\text{avg}} = (a + b)/2$, where a and b are the time differences to the next longest and next shortest observed event. Figure 1c shows the off-time and Figure 1d shows the on-time probability distributions obtained using this weighting scheme. The power-law exponents and truncation times are determined by using a least-squares method to fit the logarithm of a truncated power law to $\log[P(t_{\text{on}})]$ versus $\log[t_{\text{on}}]$. Similarly, off-time power-law exponents are determined by least-squares fitting of a straight line to $\log[P(t_{\text{off}})]$ vs. $\log[t_{\text{off}}]$. Fitting results are summarized in Figure 1c,d and complete results are given in the Supporting Information.

It has been noted that maximum-likelihood estimation has the potential to provide a more accurate analysis of blinking-time distribution functions than least-squares fitting.^{25,30} As described in the Supporting Information, we also examined the use of maximum-likelihood estimation to analyze the measured and simulated distributions. We find that the least-squares fitting and maximum-likelihood estimation give very similar results if the distributions include enough events to be considered reliable, as explained below. (We observed one discrepancy between least-squares fitting and maximum likelihood estimation that may be attributable to the distribution lacking long events, even though it has a large total number of events.)

The results for the off-time distributions confirm the findings of previous studies:^{8,12,23} changing the bin size causes the off-time distributions to shift along the time axis, but there is no change in the power-law form or the power-law exponent within confidence intervals as long as Δt is long enough that the signal and background levels can be clearly resolved in the intensity histogram.

The on-time distributions on the other hand show significant changes with rebinning. The fitted value of τ_{on} quadruples over an apparently reasonable range of Δt , the absolute value of m_{on} decreases steadily as Δt increases, and the uncertainty in m_{on} grows. Specifically, for $\Delta t = 3$ –10 ms the fitted value of τ_{on} (using the center threshold) is constant within 95 % confidence; however, for larger values of Δt the fitted value of τ_{on} and its uncertainty increase dramatically.

For $\Delta t = 1$ ms, the center threshold falls below the Poisson threshold, indicating that this binning time is too short to clearly resolve the signal and background. However, simple visual inspection of the on-time distribution (Figure 1c) and the intensity histogram (Figure 1b) does not make this clear: the on-time distribution has a reasonable shape and can be fit to a truncated power law, and the intensity histogram has a distinct two-peak structure. The value of τ_{on} obtained for $\Delta t = 1$ ms is more than a factor of 4 smaller than that obtained for $\Delta t = 3$ ms, reflecting the overlap between the background and signal.

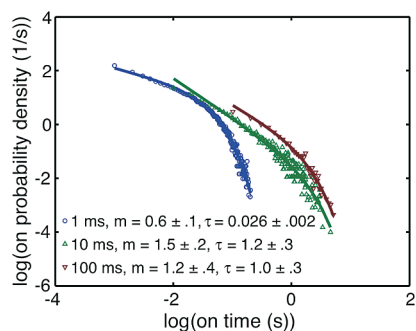


FIGURE 2. On-time probability distributions, $P(t_{\text{on}})$, obtained using center thresholding, for simulated data with a time resolution of 0.1 ms, truncation time $\tau_{\text{on}} = 1$ s, power-law exponents $m_{\text{on}} = m_{\text{off}} = 1.5$, and signal and noise levels comparable to those for the experimental data of Figure 1. Points represent the distribution obtained from the simulated data; lines are the results of least-squares fitting to these points.

The changes of the on-time distributions with binning time are largely reproduced in a simulation that employs a simple, two-state blinking model, indicating that the binning dependence is primarily an artifact of the data analysis. We construct a time series by assuming that the nanocrystal switches randomly between a bright state and a dark state with off times selected from a power-law distribution and on times from a truncated power-law distribution. We add Poisson-distributed noise (shot noise) to the simulated time series with the amplitudes of signal and noise chosen to match the data shown in Figure 1. Details on the simulation method are given in the Supporting Information. Figure 2 shows the on-time distributions obtained from simulated data for $\Delta t = 1$ –100 ms. The parameters determined by least-squares fitting, using the center threshold, are summarized in the figure, and further details of the fits are given in the Supporting Information. For $\Delta t = 1$ ms, the fitted parameters do not match the input values for the simulation at all, because the signal and background are not clearly distinguishable. For $\Delta t \geq 3$ ms, we observe the same trend of the declining power law exponent and increasing uncertainty as for the experimental data. Simulations without the added noise show nearly identical fitted parameter values and uncertainties for $\Delta t \geq 3$ ms (see the Supporting Information for details).

The simulations also demonstrate that long measurements with a large number of observed blinking events are required to accurately determine the distribution parameters. Accurate determination of a truncated-power-law distribution, or even a simple power-law distribution, requires that the distribution span many decades in time. In fact, it is difficult to even distinguish a power-law distribution from other types of distributions unless three or more decades are measured.³¹ This, in turn, requires an extended measurement in order to observe a sufficient number of long blinking events. In order to analyze the effect of experiment duration, we simulated data corresponding to a 20,000 s measurement (far longer than most reported measurements

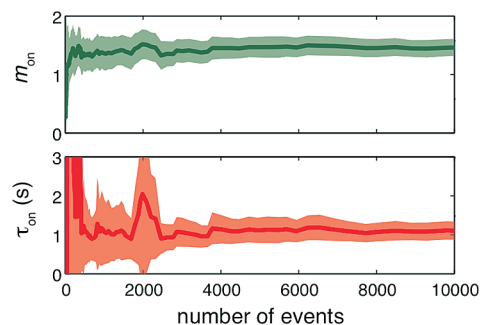


FIGURE 3. Dependence of exponent, m_{on} , and truncation time, τ_{on} , on number of on-events in intensity trajectory for simulated data with Poisson noise with same simulation parameters (other than duration) as Figure 2, using $\Delta t = 10$ ms, least-squares fitting, and center threshold. Solid lines indicate fitted parameter values; shaded regions indicate 95% confidence intervals.

of blinking), corresponding to approximately 40,000 events. We then analyzed segments of that simulation with different lengths (all taken from the beginning of the simulation). Figure 3 shows the resulting dependence of the fitted parameters on the number of observed blinking events, for $\Delta t = 10$ ms. The values of the fitted parameters are relatively steady for segments with approximately 4000 events or more, corresponding to about 2000 s. However, for segments with fewer events, the fit parameters begin to vary more dramatically and the uncertainties also grow significantly as the number of events decreases; for segments with fewer than about 2500 events, the uncertainties become so great that the fits are unlikely to be meaningful. For different values of Δt , similar trends are observed. Similarly, the Figure 1 data, when analyzed with $\Delta t = 30$ ms, has fewer than 2000 events in the probability distribution, and the on-time distribution shows significant distortion, even though one might expect this Δt to be sufficiently short compared to the truncation time to give good results.

As has previously been demonstrated, with a fixed binning time the threshold, I_{th} , can be varied over a few standard deviations of the background, consistent with the different choices generally employed in the literature, without significantly affecting trends in the on-time distributions.^{14,18} If, for example, we use the Poisson threshold rather than the center threshold for the experimental data, the fitted truncation times, τ_{on} , show the same trend with bin time (as long as the bin time is large enough that the signal and background are resolved). For the simulated data, using the Poisson threshold likewise gives a more rapidly declining exponent with increasing bin time, but an equally good match to the simulated τ_{on} . By varying I_{th} over a wider range, as illustrated in Figure 4a for $\Delta t = 3$ ms, we see that τ_{on} is stable if I_{th} falls in the flat region between the background and signal peaks in the intensity histogram.

On the other hand, significant distortions in the on-time distributions occur if I_{th} falls outside of this range;²⁵ τ_{on} increases substantially if the threshold falls within the background and decreases substantially if the threshold falls

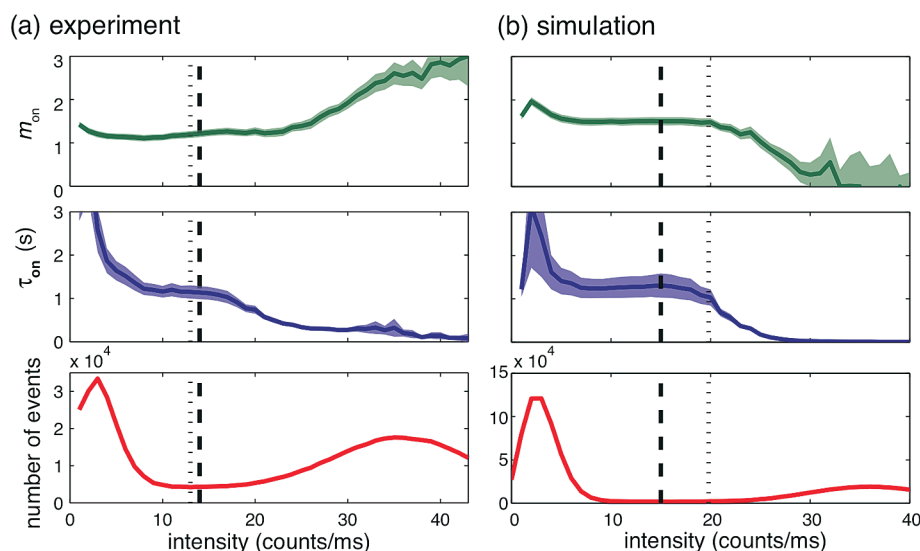


FIGURE 4. (a) Dependence of exponent, m_{on} , and truncation time, τ_{on} , on threshold, I_{th} , for the experimental data shown in Figure 1, binned with $\Delta t = 3$ ms, using least-squares fitting. (b) Dependence of m_{on} and τ_{on} , on I_{th} for the on-time distribution from the simulated data shown in Figure 2, using the same binning and fitting. For all panels, solid lines indicate parameter values and shaded regions indicate 95% confidence intervals. Intensity histograms with center and Poisson thresholds indicated are shown for reference in the bottom panels.

within the signal peak. The exponent, m_{on} , is stable for threshold values up to the signal peak, and then begins to climb for higher threshold values. The simulated data with noise show similar threshold dependence for τ_{on} , as shown in Figure 4b. The value of m_{on} from simulations likewise shows a threshold dependence similar to the experimental data for I_{th} up to approximately half the maximum measured intensity; for larger thresholds, the simulated m_{on} begins to decline, in contrast to the experimental result. This indicates that the simulations accurately reproduce the general characteristics of the experimental data and their sensitivity to binning and thresholding but suggests that there are additional fluctuations in the bright states of real nanocrystals that are not described by the simple model of a two-state system with Poisson noise.

For the data shown in Figure 1, these additional fluctuations are small enough that it is still possible to treat the data as if it consisted of only a single bright state and a single dark state and extract, for certain binning times and thresholds, meaningful on-time and off-time distributions. This is true for the majority of the core-shell nanocrystals that we studied; a second representative example is given in the Supporting Information. However, for a small fraction of the nanocrystals and for all of the nanorods studied, the intensity histograms did not show two distinct peaks for any Δt , even though distinct dark periods are visible in $I(t)$. Figure 5 shows an example of such data from a single nanorod.

In this case, a center threshold cannot be defined, so we can use only the Poisson threshold. Again, the off-time distributions are not affected by binning, but the on-time distributions are; such data sets show steady, substantial decrease in m_{on} and increase in τ_{on} as Δt increases, as shown in Figure 5c. Figure 5d shows the variation of fitting parameters with threshold for $\Delta t = 10$ ms; τ_{on} , in particular, varies

continuously with I_{th} . For such data, a binning-independent of-time distribution cannot be determined.

We attempted to modify our simulations in order to produce intensity trajectories with single-peak intensity histograms. In order to obtain a histogram without a clear two-peak structure from a simulation of a two-state system, it is necessary either that the signal-to-noise ratio is low, so that there is substantial overlap between the background and signal peaks, or else τ_{on} is very short, so that the signal peak is spread out and no longer follows Poisson statistics. Simulating data with a low signal level but with long τ_{on} (100 ms or greater) gives a histogram without a distinct second peak but also without the long tail at high intensities that is observed in the experimental data. Simulating data with very short τ_{on} gives an intensity histogram with a clear transition between a narrow background peak and an extended, overlapping on-state peak, unlike the smooth peak with a broad tail that is seen for the experimental data.

This suggests that emission from these nanoparticles involves more than just a single bright state and a single dark state. Indeed, other methods of analyzing NC emission have indicated the presence of multiple bright states.^{32,33} Yang and co-workers have applied a changepoint analysis method to analyze the statistics of switching among these many levels.³⁴ This alternative method avoids binning the data and applying a threshold and may thus avoid many of the difficulties discussed here.³⁵ Nonetheless, the changepoint method involves various explicit and implicit assumptions, and a detailed analysis of potential artifacts is still needed. Alternative statistical analysis methods, particularly calculation of autocorrelation functions^{18,36–39} or power spectral densities,^{40,41} can be performed directly on the raw data without requiring arbitrary assumptions. The trade-off for this is generally a reduced amount of information; power

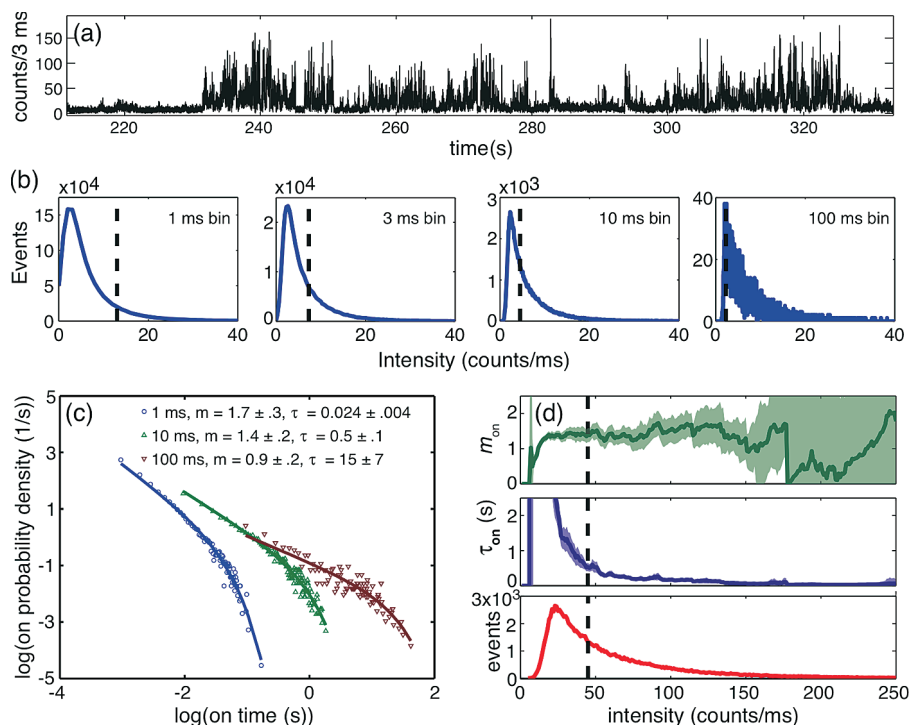


FIGURE 5. (a) Representative excerpt from an intensity time trace, $I(t)$, obtained from a single nanorod, using binning time $\Delta t = 3$ ms. The total duration of the experiment was 1200 s. (b) Histograms of intensities obtained from entire duration of the data set excerpted in (a), for $\Delta t = 1, 3, 10$, and 100 ms. The Poisson threshold is shown by the heavy dashed line. (c) On-time probability distributions, $P(t_{\text{on}})$, obtained using the Poisson threshold, for different values of Δt . Points are experimental values, and lines are the results of least-squares fitting. (d) Dependence of power-law exponent m_{on} , and truncation time, τ_{on} , on threshold, I_{th} , using $\Delta t = 10$ ms. Solid lines are parameter values and shaded lines indicate 95% confidence intervals. The intensity histogram is shown, for reference, in the bottom panel.

spectra, for example, cannot provide independent information about bright and dark states.

In summary, our simulations and experimental data show that on-time distributions for blinking quantum dots are described by a truncated power law whose apparent exponent, m_{on} , and truncation time, τ_{on} , can be strongly affected by the choice of binning time, Δt , and threshold, I_{th} , in the data analysis. If Δt is too small, the signal-to-noise ratio is insufficient to allow the on states and off states to be clearly distinguished from one another. If Δt is too large, on the other hand, multiple blinking events are likely to occur during a single binning period, distorting the probability distributions. In addition, even an appropriate choice of Δt may not allow accurate determination of the probability distributions if the experiment is too short and too few blinking events are recorded.

Our findings suggest that rather stringent experimental criteria must be met in order that useful probability distributions can be recovered. Specifically, experimental data should be rebinned using a large range of binning times, Δt . Any particular value of Δt has the potential to produce a meaningful blinking-time distribution only if (1) the calculated intensity histogram exhibits clear, nonoverlapping peaks reflecting bright and dark states, and (2) the time trajectory includes several thousand blinking events. If these criteria are met for at least a decade of different Δt values, the resulting blinking-time distributions can be analyzed

using least-squares fitting or maximum-likelihood estimation. If the fitted exponent, m_{on} , and truncation time, τ_{on} , are consistent over a range of values of Δt , and if the apparent value of τ_{on} is at least 10 times greater than the largest Δt used, then the fitting results can be considered reliable.

Although in practice it is challenging and therefore rare to measure intensity trajectories for well over 1200 s, our results suggest that experimental durations of at least 2000 s may be required in order to accumulate enough blinking events, and even longer measurements may be required if τ_{on} is greater than 1 s. It is also a significant experimental challenge to obtain data with signal-to-noise ratio high enough that binning can reliably be performed over a decade of Δt values. Among 14 data sets that we obtained from single NCs, only four allowed for the accurate determination of τ_{on} according to our criteria. These were the data sets with the highest count rates, which raises the issue of whether selecting data that can be analyzed in this manner biases the analysis toward the brightest NCs. Furthermore, increasing the excitation rate in order to boost the count rate has been observed to decrease τ_{on} .¹⁵ In their recent study of the excitation rate dependence of blinking statistics,¹⁵ Peterson and Nesbitt reported an unusually high signal-to-noise ratio, which allowed them to use $\Delta t = 1$ ms; most of their study was performed using very high excitation rates, and the truncation times they report are 2.5 s or less. This suggests that accurately measuring longer truncation times, which

most likely correspond to lower excitation rates, may be very difficult. Many reported values of τ_{on} are substantially longer^{10,18–21} and may be affected by these considerations.

Although our work has focused on semiconductor nanocrystals, many other single fluorophores also display complex blinking behavior, including certain fluorescent molecules, fluorescent proteins, and polymer segments.² Our results indicate that care must be taken in analyzing such data in order to ensure that the measured statistics are not distorted by the choice of binning time. Furthermore, a wide range of electrical and optical phenomena display switching; the considerations explored here apply to any time series data that displays apparent telegraph noise.

Acknowledgment. This work was supported by the HHMI grant to Swarthmore College for undergraduate summer research; partial support at the University of Pennsylvania was provided by the NSF Career Award DMR-0449533 and ONR YIP N000140410489. Work at the Center for Nanoscale Materials was supported by the U.S. Department of Energy, Office of Science, Office of Basic Energy Sciences, under Contract No. DE-AC02-06CH11357. We thank Philip Everson and Eric Jensen for advice on statistical analysis, Pavel Frantsuzov and colleagues for advice on the maximum likelihood method, Jack Harris for bringing reference 24 to our attention, and Siying Wang and Tali Dadosh for helpful feedback on the results and the manuscript. Simulations made use of Matlab codes placed in the public domain by Aaron Clauset (more details in Supporting Information).

Supporting Information Available. Experimental methods, simulation methods, detailed results of experimental data analysis, and detailed results of simulated data analysis. This material is available free of charge via the Internet at <http://pubs.acs.org>.

REFERENCES AND NOTES

- Cichos, F.; von Borczyskowski, C.; Orrit, M. *Curr. Opin. Colloid Interface Sci.* **2007**, *12*, 272–284.
- Frantsuzov, P.; Kuno, M.; Janko, B.; Marcus, R. A. *Nat. Phys.* **2008**, *4*, 519–522.
- Stefani, F.; Hoogenboom, J.; Barkai, E. *Phys. Today* **2009**, *62*, 34–39.
- Chen, Y.; Vela, J.; Htoon, H.; Casson, J. L.; Werder, D. J.; Bussian, D. A.; Klimov, V. I.; Hollingsworth, J. A. *J. Am. Chem. Soc.* **2008**, *130*, 5026–5027.
- Mahler, B.; Spinicelli, P.; Buil, B.; Quelin, X.; Hermier, J.-P.; Dubertret, B. *Nat. Mater.* **2008**, *7*, 659–664.
- Wang, X.; Ren, X.; Kahen, K.; Hahn, M.; Rajeswaran, M.; MacCagnano-Zacher, S.; Silcox, J.; Cragg, G.; Efros, A.; Krauss, T. *Nature* **2009**, *459*, 686–689.
- Kuno, M.; Fromm, D. P.; Hamann, H. F.; Gallagher, A.; Nesbitt, D. J. *J. Chem. Phys.* **2000**, *112*, 3117–3120.
- Kuno, M.; Fromm, D. P.; Hamann, H. F.; Gallagher, A.; Nesbitt, D. J. *J. Chem. Phys.* **2001**, *115*, 1028–1040.
- Kuno, M.; Fromm, D. P.; Johnson, S. T.; Gallagher, A.; Nesbitt, D. J. *Phys. Rev. B* **2003**, *67*, 125304.
- Shimizu, K. T.; Neuhauser, R. G.; Leatherdale, C. A.; Empedocles, S. A.; Woo, W. K.; Bawendi, M. G. *Phys. Rev. B* **2001**, *63*, 205316.
- Nirmal, M.; Dabbousi, B. O.; Bawendi, M. G.; Trautman, J. K.; Garris, T. D.; Brus, L. E. *Nature* **1996**, *383*, 802–804.
- Chung, I. H.; Bawendi, M. G. *Phys. Rev. B* **2004**, *70*, 165304.
- Stefani, F.; Knoll, W.; Kreiter, M.; Zhong, X.; Han, M. *Phys. Rev. B* **2005**, *72*, 125304.
- Wang, S.; Querner, C.; Emmons, T.; Drndic, M.; Crouch, C. H. *J. Phys. Chem. B* **2006**, *110*, 23221–23227.
- Peterson, J.; Nesbitt, D. *Nano Lett.* **2009**, *9*, 338–345.
- Lee, D.-H.; Yuan, C.-T.; Tachiya, M.; Tang, J. *Appl. Phys. Lett.* **2009**, *95*, 163101.
- Goushi, K.; Yamada, T.; Otomo, A. *J. Phys. Chem. C* **2009**, *113*, 20161–20168.
- Wang, S.; Querner, C.; Fishbein, M. D.; Willis, L.; Novikov, D. S.; Crouch, C. H.; Drndic, M. *Nano Lett.* **2008**, *8*, 4020–4026.
- Knappenberger, K. L.; Wong, D. B.; Romanyuk, Y. E.; Leone, S. R. *Nano Lett.* **2007**, *7*, 3869–3874.
- Knappenberger, K. L.; Wong, D. B.; Xu, W.; Schwartzberg, A. M.; Wolcott, A.; Zhang, J. Z.; Leone, S. R. *ACS Nano* **2008**, *2*, 2143–2153.
- Crouch, C. H.; Mohr, R.; Emmons, T.; Wang, S.; Drndic, M. *J. Phys. Chem. C* **2009**, *113*, 12059–12066.
- Watkins, L. P.; Yang, H. *J. Phys. Chem. B* **2005**, *109*, 617–628.
- Lippitz, M.; Kulzer, F.; Orrit, M. *ChemPhysChem* **2005**, *6*, 770–789.
- Naaman, O.; Aumentado, J. *Phys. Rev. Lett.* **2006**, *96*, 100201.
- Stefani, F.; Zhong, X.; Knoll, W.; Han, M.; Kreiter, M. *New J. Phys.* **2005**, *7*, 197.
- Krogmeier, J.; Hwang, J. *Proc. SPIE* **2005**, *5705*, 255–262.
- Frantsuzov, P. A.; Volkán-Kacsó, S.; Jankó, B. *Phys. Rev. Lett.* **2009**, *103*, 207402.
- Many reports in the literature do not make clear how I_{th} was chosen; inspection of the data provided in these papers suggests that variations on the “center threshold” and standard deviation-based threshold approaches are common.
- Peck, K.; Stryer, L.; Glazer, A. N.; Mathies, R. A. *Proc. Natl. Acad. Sci. U.S.A.* **1989**, *86*, 4087–4091.
- Hoogenboom, J.; den Otter, W.; Offerhaus, H. J. *Chem. Phys.* **2006**, *125*, 204713.
- Clauset, A.; Shalizi, C. R.; Newman, M. E. J. *SIAM Rev.* **2009**, *51*, 661.
- Schlegel, G.; Bohnenberger, J.; Potapova, I.; Mews, A. *Phys. Rev. Lett.* **2002**, *88*, 137401.
- Fisher, B. R.; Eisler, H. J.; Stott, N. E.; Bawendi, M. G. *J. Phys. Chem. B* **2004**, *108*, 143–148.
- Zhang, K.; Chang, H.; Fu, A.; Alivisatos, A. P.; Yang, H. *Nano Lett.* **2006**, *6*, 843–847.
- Wustholz, K. L.; Bott, E. D.; Kahr, B.; Reid, P. J. *J. Phys. Chem. C* **2008**, *112*, 7877–7885.
- Messin, G.; Hermier, H. P.; Giacobino, E.; Desbiolles, P.; Dahan, M. *Opt. Lett.* **2001**, *26*, 1891–1893.
- Larson, D. R.; Zipfel, W. R.; Williams, R. M.; Clark, S. W.; Bruchez, M. P.; Wise, F. W.; Webb, W. W. *Science* **2003**, *300*, 1434–1436.
- Yao, J.; Larson, D. R.; Vishwasrao, H. D.; Zipfel, W. R.; Webb, W. W. *Proc. Natl. Acad. Sci. U.S.A.* **2005**, *102*, 14284–14289.
- Yu, M.; van Orden, A. *Phys. Rev. Lett.* **2006**, *97*, 237402.
- Pelton, M.; Grier, D. G.; Guyot-Sionnest, P. *Appl. Phys. Lett.* **2004**, *85*, 819–821.
- Pelton, M.; Smith, G.; Scherer, N. F.; Marcus, R. A. *Proc. Natl. Acad. Sci. U.S.A.* **2007**, *104*, 14249–14254.